Inosine, but none of the 8-oxo-purines, is a plausible component of a primordial version of RNA

Seohyun Chris Kim[a], Derek K. O'Flaherty[b,c,d], Lijun Zhou[b,c,d], Victor S. Lelyveld[b,c,d], and Jack W. Szostak[a,b,c,d,1]

[a]Department of Chemistry and Chemical Biology, Harvard University, Cambridge, MA 02138; [b]Howard Hughes Medical Institute, Massachusetts General Hospital, Boston, MA 02114; [c]Department of Molecular Biology, Center for Computational and Integrative Biology, Massachusetts General Hospital, Boston, MA 02114; and [d]Department of Genetics, Harvard Medical School, Boston, MA 02115

Edited by Gerald F. Joyce, The Salk Institute, La Jolla, CA, and approved October 26, 2018 (received for review August 21, 2018)

The emergence of primordial RNA-based life would have required the abiotic synthesis of nucleotides, and their participation in nonenzymatic RNA replication. Although considerable progress has been made toward potentially prebiotic syntheses of the pyrimidine nucleotides (C and U) and their 2-thio variants, efficient routes to the canonical purine nucleotides (A and G) remain elusive. Reported syntheses are low yielding and generate a large number of undesired side products. Recently, a potentially prebiotic pathway to 8-oxo-adenosine and 8-oxo-inosine has been demonstrated, raising the question of the suitability of the 8-oxo-purines as substrates for prebiotic RNA replication. Here we show that the 8-oxo-purine nucleotides are poor substrates for nonenzymatic RNA primer extension, both as activated monomers and when present in the template strand; their presence at the end of a primer also strongly reduces the rate and fidelity of primer extension. To provide a proper comparison with 8-oxo-inosine, we also examined primer extension reactions with inosine, and found that inosine exhibits surprisingly rapid and accurate nonenzymatic RNA copying. We propose that inosine, which can be derived from adenosine by deamination, could have acted as a surrogate for G in the earliest stages of the emergence of life.

origin of life | RNA replication | primordial RNA

The nature of the primordial genetic polymer of life is a subject of continuing debate. Although there is strong evidence in support of an early stage in the evolution of life, during which RNA played dual roles as both a genetic and a functional polymer (1–3), the question of possible progenitors to RNA remains unresolved. At one extreme is the idea that life began with a much simpler genetic polymer, such as might be formed from the self-assembling melamine:barbituric acid nucleotides, studied by Hud and coworkers (4). However, informational inheritance has not yet been demonstrated in such simple systems, and how such systems could transition to more modern genetic polymers found in nature is unclear. At the other extreme lies the conceptually simple idea that life began with essentially modern RNA, synthesized directly by prebiotic chemical processes. This model, championed by Sutherland, is supported by the demonstration of potentially prebiotic pathways to the canonical pyrimidine nucleotides (5, 6), but purine nucleotide synthesis remains challenging (7). Furthermore, despite recent advances, the nonenzymatic replication of RNA is still an unsolved problem (8). Between these two extremes lie many models that suggest that the primordial polymer was closely related to, but not identical to, modern RNA. Many of these models invoke a degree of heterogeneity in the backbone (e.g., a mixture of 2′-5′ and 3′-5′ linkages) (9), in the sugar (e.g., a mixture of 2′-deoxyribose and ribose) (10), or in the nucleobases, which might have been partially or fully replaced with modified nucleobases such as 2-thio-uracil to provide stronger and more accurate base-pairing (11). Because a major goal of research into the origin of life is to delineate plausible pathways from prebiotic chemistry to simple forms of life, continued investigation of the chemistry of potential early genetic polymers is needed to bring to the forefront chemical variations on RNA that could have been involved in the origin of life, while eliminating nonfunctional chemistry from consideration. Here we show that the 8-oxo-purine nucleotides, recently shown to be potential products of prebiotic chemical pathways (7), could not have been part of a primordial RNA-like genetic polymer, whereas inosine, previously dismissed as a plausible substitute for guanosine (12, 13), functions as well as guanosine in an experimental model of RNA copying chemistry.

Because there were no evolved macromolecular catalysts such as enzymes or ribozymes at the earliest stages of the origin of life, both the rate and fidelity of nonenzymatic replication are of special interest (8, 14). Since RNA is easily degraded, nonenzymatic replication cannot be arbitrarily slow. Similarly, the error rate of nonenzymatic RNA replication must not exceed the Eigen error threshold (roughly the reciprocal of the number of critical bases in a sequence), above which genetic information cannot be maintained because mutations accumulate faster than they can be eliminated by selection (15). Small ribozymes with catalytic rates on the order of 1 min^{-1} are typically at least 30–50 nucleotides in length (16), suggesting that an error rate of less than 2–3% would be necessary to preserve functional information during repeated cycles of replication (17). Modern cellular life employs highly evolved polymerases and error-correcting enzymatic pathways to ensure high fidelity (18, 19); primitive

Significance

The RNA world hypothesis assumes the abiotic synthesis of nucleotides, as well as their participation in nonenzymatic RNA replication. Whereas prebiotic syntheses of the canonical purine nucleotides remain inefficient, a prebiotically plausible route to the 8-oxo-purines has been reported. Although these noncanonical purine nucleotides are known to engage in non-Watson–Crick pairing with their canonical purine counterparts, their behavior in nonenzymatic RNA copying has not been evaluated. Our study indicates that none of the 8-oxo-purines behaves as a suitable substrate for nonenzymatic RNA copying. However, inosine turns out to exhibit reasonable rates and fidelities in RNA copying reactions. We propose that inosine could have served as a surrogate for guanosine in the early emergence of life.

Author contributions: S.C.K., D.K.O., L.Z., and J.W.S. designed research; S.C.K., D.K.O., and L.Z. performed research; L.Z. contributed new reagents/analytic tools; S.C.K., D.K.O., V.S.L., and J.W.S. analyzed data; and S.C.K., D.K.O., L.Z., V.S.L., and J.W.S. wrote the paper.

The authors declare no conflict of interest.

This article is a PNAS Direct Submission.

[1]To whom correspondence should be addressed. Email: szostak@molbio.mgh.harvard.edu.

This article contains supporting information online at www.pnas.org/lookup/suppl/doi:10.1073/pnas.1814367115/-/DCSupplemental.

Published online December 3, 2018.

protocells, in contrast, could only have relied on the intrinsic chemical properties of nonenzymatic RNA polymerization to govern the fidelity of heredity before the advent of enzymatic mechanisms to survey and correct errors. Nonenzymatic template-directed RNA synthesis has been reported to show error rates of up to 17%, with most errors arising from G:U wobble pairing (20). However, the significant decrease in the rate of continued RNA primer extension after a mismatched base pair, referred to as the stalling effect, increases the effective fidelity of the most rapidly synthesized full-length products (15). Elucidating the parameters that govern fidelity, rate, and stalling factors is therefore critical in evaluating the prebiotic conditions that would favor the emergence of Darwinian evolution.

The kinetics and fidelity of nonenzymatic copying reactions can be improved with modified nucleobases. For example, higher fidelity can be achieved by substituting 2-thio-uridine (s^2U) or 2-thio-ribothymidine (s^2rT) for U, which simultaneously stabilizes the correct A:U base pair and destabilizes the undesired G:U wobble pair (11, 21). In contrast, the deamination of adenosine yields inosine, which can pair with a number of nucleobases (A, U, and C) (22), and which might therefore be expected to exhibit low fidelity in copying reactions. The 8-oxo-purines, which arise from oxidative damage, tend to adopt a *syn* conformation and form Hoogsteen base pairs, which may also decrease copying fidelity (Fig. 1) (23, 24). It is reasonable to assume that prebiotic synthetic pathways that generate nucleotides may also yield intermediates and byproducts, or damage and decay products, that give rise to non-Watson–Crick base pairs. Indeed, recent advances by Powner and coworkers (7) demonstrate efficient prebiotic pathways to the 8-oxo-purine nucleotides and the pyrimidine nucleotides that diverge from a common precursor. As the effects of the 8-oxo-purine and inosine nucleotides on the fidelity and kinetics of nonenzymatic RNA copying have not previously been explored, we sought to evaluate 8-oxo-purines and inosine as potential prebiotic surrogates for the canonical purines.

Given the significance of prebiotic synthetic pathways, as well as the unusual pairing properties of 8-oxo-purines and inosine, we sought to evaluate how these noncanonical nucleotides behave when used in place of the canonical nucleotides in nonenzymatic, template-directed primer extension reactions. We find that activated 8-oxo-purine monomers show extremely low rates of primer extension, and once incorporated, they strongly decrease the rate of incorporation of the next nucleotide. Furthermore, 8-oxo-purine nucleotides on the template strand lower the fidelity by promoting primer extension with both Watson–Crick and Hoogsteen pairing partners. However, activated inosine monomers can be incorporated at a rate comparable to activated guanosine opposite C in the template, while minimally affecting subsequent primer extension. In addition, inosine in the template strand promotes rapid primer extension with cytidine, suggesting that inosine would be an effective component of a primitive genetic polymer.

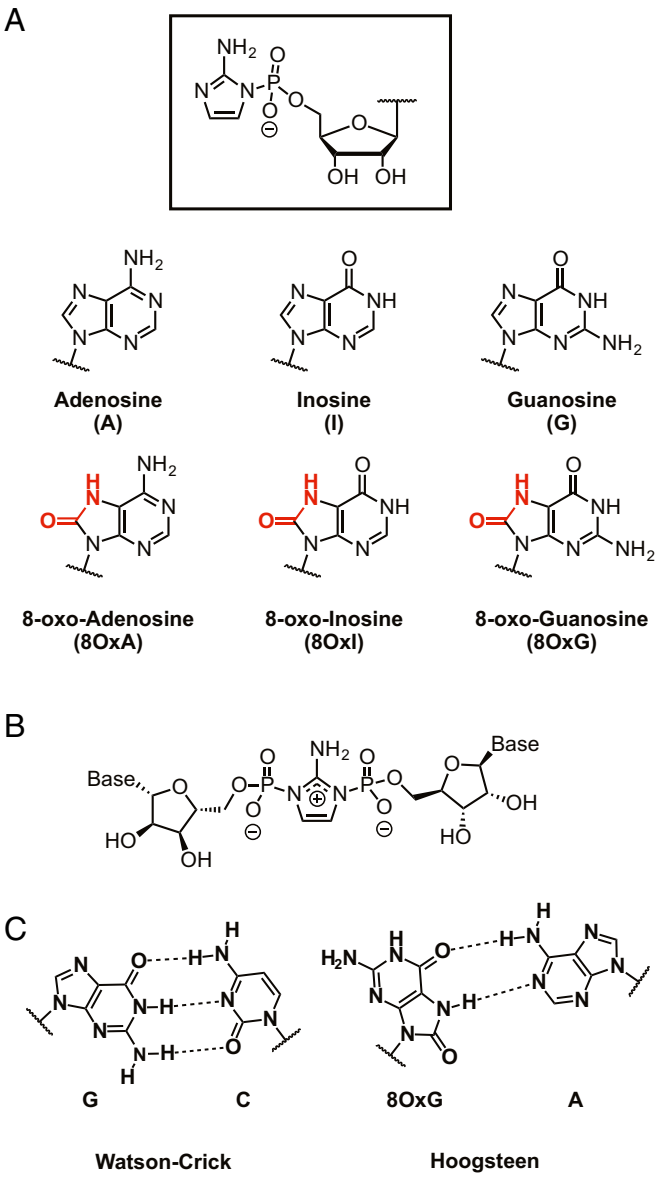

Fig. 1. (*A*) Chemical structures of 2-amino-imidazole activated purine and 8-oxo-purine nucleotides. (*B*) Chemical structure of reactive 2-amino-imidazolium-bridged intermediate in template-directed primer extension. (*C*) Chemical structures of Watson–Crick pairing (*Left*, e.g., G:C) and Hoogsteen pairing (*Right*, e.g., 8OxG:A).

Results

Primer Extension with 8-Oxo-Purine Monomers. To investigate the activity of the 8-oxo-purine nucleotides as substrates for nonenzymatic primer extension, we evaluated the rate of primer extension using these noncanonical nucleotides as activated monomers across from all four canonical nucleotides on a series of templates (Fig. 2). Our laboratory has previously shown that 5′-activated downstream oligonucleotides significantly accelerate primer extension with activated monomers, such that an RNA template with all four canonical nucleobases can be copied (25). This catalytic effect is the result of the reaction of the incoming activated monomer with the activated downstream oligonucleotide to form a highly preorganized imidazolium-bridged species that is poised to react with the primer (26). Structural stabilization of the correct helical geometry by the downstream helper oligonucleotide also contributes to the overall rate enhancement (27). We therefore prepared 2-aminoimidazole (2AI) activated 5′-monophosphates of 8-oxo-A (8OxA), 8-oxo-G (8OxG), and 8-oxo-I (8OxI) to give the corresponding activated monomers 2AIp-8OxA, 2AIp-8OxG, and 2AIp-8OxI, respectively (Fig. 1) (28). We also generated a 2AI-activated trinucleotide helper, and we used this downstream trinucleotide in all experiments where we measured the kinetics of monomer incorporation in helper-assisted nonenzymatic primer extension reactions (Fig. 2*A*).

The observed rate of primer extension for each activated monomer was compared with that of the canonical activated monomers (A, U, G, or C; Fig. 2 *B* and *C*) across from their Watson–Crick pairing partners on the template (Fig. 2*B*). The observed rates (k_{obs}) varied over three orders of magnitude, indicating that, as expected, the identity of the nucleobase plays a critical role in the rate of template-directed primer extension.

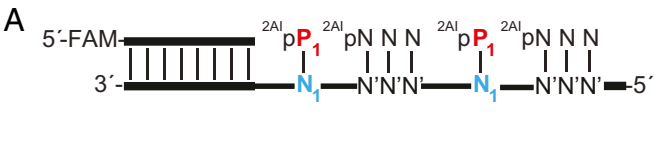

Copying rate k_{obs} (h^{-1})

B

N_1 \ P_1	8OxA	8OxG	8OxI	W.C.
A	0.00075(9)	0.040(2)	0.00083(7)	6.2(2)
U	0.0036(4)	0.040(9)	0.00042(3)	3.1(1)
G	0.0010(1)	0.0052(4)	0.00089(6)	10.2(2)
C	0.0091(5)	0.0081(4)	0.0075(7)	11.7(5)

C

N_1 \ P_1	A	U	G	C	μ_N
8OxG	4.0(1)	0.045(2)	0.85(7)	4.1(1)	0.54
G	0.0025(1)	0.075(2)	0.040(9)	10.2(2)	0.011
8OxA	0.12(2)	2.1(1)	0.34(1)	0.019(4)	0.19
A	0.013(4)	6.2(2)	0.0021(1)	0.11(3)	0.020

Fig. 2. Evaluation of 8-oxo-purine nucleotides in nonenzymatic primer extension. All reactions were performed at pH 8.0, 200 mM Na-Hepes, 50 mM Mg^{2+}, 20 mM $2AIpP_1$, 0.5 mM activated trimer. (*A*) Schematic representation of a primer extension reaction. $2AIpP_1$ represents 2-aminoimidazole-activated monomers, and 2AIpNNN represents 2-aminoimidazole-activated trimer helper. (*B*) Rates of primer extension for 2-aminoimidazole-activated 8-oxo-purines across canonical nucleotides. W.C. indicates the Watson–Crick pair monomer corresponding to each nucleobase on template. (*C*) Rates of primer extension for 2-aminoimidazole-activated canonical nucleotides across 8-oxo-purine nucleotides. Projected misincorporation rates (μ_N) for template bases N_1 were determined by dividing the sum of the incorporation rates across the incorrect pairs by the sum of all the incorporation rates across represented P1 bases. See *SI Appendix* for kinetic analysis of primer extension reactions (*SI Appendix*, Figs. S1–S7). Values are reported as the mean +/− SD from triplicate experiments.

Activated canonical monomers that form Watson–Crick base pairs with the template exhibited rates of primer extension ranging from 3.1 to 11.7 h^{-1}. The activated 8-oxo-purine monomers exhibited drastically slower rates of primer extension across from all the canonical nucleotides. Although addition rates of the 8-oxo-purine monomers opposite Watson–Crick pairing partners were higher than their addition rates when opposite Hoogsteen pairing partners, both were at least 100-fold slower than that of the standard purine monomers with Watson–Crick pairing to the template. Overall, 2AIp-8-oxo-purines were incorporated at rates similar to those of the canonical nucleotides when mismatched with the template.

Primer Extension Across 8-Oxo-Purines in the Template Strand. Although templates containing 8-oxo-purines would only rarely be generated by the copying chemistry described earlier, they could potentially be generated by the nontemplated polymerization of activated monomers (e.g., in ice eutectic phases). In addition, the 8-position of purines is susceptible to oxidative damage, suggesting that 8-oxo-purine-containing templates could be generated by radical oxidation of the parent nucleobases (29) (e.g., in environments subject to high levels of radiation). We therefore examined the effects of 8-oxo-purine nucleotides at internal positions in the template strand (Fig. 2*C*). To measure the rates of primer extension with activated canonical nucleotides (2AIpN) across from template sites consisting of 8-oxo-purine nucleotides (Fig. 2*C*), we prepared RNA templates containing 8-oxo-A and 8-oxo-G by solid phase synthesis. Intriguingly, 8-oxo-G-containing templates show high rates of primer extension with both activated C and A monomers (~4 h^{-1}); whereas the 2AIp-8-oxo-G incorporation rate was almost negligible across from either C or A in the template (<0.05 h^{-1}). Compared with the corresponding canonical purines, 8-oxo-purine templates have lower rates of primer extension with Watson–Crick pairing monomers, whereas they have much higher rates for Hoogsteen pairing monomers (8OxG:A and 8OxA:G). Thus, the estimated error rates for the copying of 8-oxo-purines in a template were quite high, with $\mu_{8OxG} = 0.54$ and $\mu_{8OxA} = 0.19$ (Fig. 2*C*).

Primer Extension with Inosine as Monomer and in the Template. As a control for comparison with 8-oxo-inosine, and to further examine the competency of noncanonical nucleobases in nonenzymatic primer extension, we evaluated the rates of primer extension using inosine in nonenzymatic primer extension reactions (Fig. 3*A*). We used the same reaction conditions as used previously in evaluating activated 8-oxo-purine monomers to measure the addition of 2AIpI across from A, U, G, C, and I on the template (Fig. 3*B*). Unlike activated 8-oxo-purine monomers, the inosine monomer showed a high rate of primer extension (6.4 h^{-1}) when paired with cytosine in the template. Of note, this rate was faster than the rate of A addition when paired

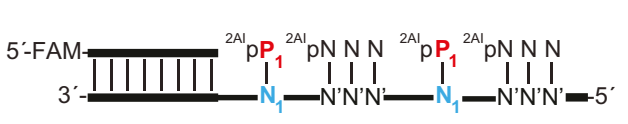

B

N_1 \ P_1	A	U	C	I	μ_N
A	0.013(4)	6.2(2)	0.11(3)	0.024(1)	0.023
U	3.1(1)	0.17(1)	0.034(3)	0.17(1)	0.11
C	0.17(2)	0.065(3)	0.16(1)	6.4(7)	0.058
I	0.05(1)	0.015(1)	8.0(5)	0.0070(1)	0.0089
				μ_{avg}	0.049

C

N_1 \ P_1	A	U	C	G	μ_N
A	0.013(4)	6.2(2)	0.11(3)	0.0021(1)	0.020
U	3.1(1)	0.17(1)	0.034(3)	0.58(2)	0.20
C	0.17(2)	0.065(3)	0.16(1)	11.7(5)	0.033
G	0.0025(1)	0.075(2)	10.2(2)	0.040(9)	0.011
				μ_{avg}	0.066

Fig. 3. Evaluation of inosine nucleotide in nonenzymatic primer extension. (*A*) Schematic representation of a primer extension reaction. $2AIpP_1$ represents 2-aminoimidazole-activated monomers, and 2AIpNNN represents 2-aminoimidazole-activated trimer helper. (*B*) Rates of primer extension for $2AIpP_1$ across A, U, C, and I. Projected misincorporation rates (μ_N) for template bases N_1 were determined by dividing the sum of the incorporation rates across the incorrect pairs by the sum of all of the incorporation rates across represented P_1 bases. (*C*) Rates of primer extension for $2AIpP_1$ across A, U, C, and G. Projected misincorporation rates (μN) were determined analogously as in *B*, with G replacing I. All reactions were performed at pH 8.0, 200 mM Hepes, 50 mM Mg^{2+}, 20 mM 2AIpP1, 0.5 mM of activated trimer. See *SI Appendix* for kinetic analysis of primer extension reactions (*SI Appendix*, Figs. S8–S10). Values are reported as the mean +/− SD from triplicate experiments.

A

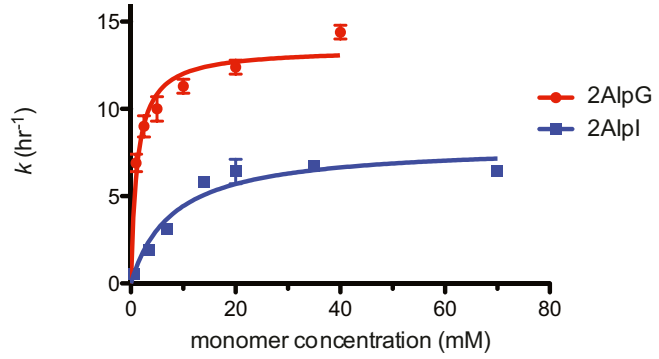

B

	V_{max} (mM h^{-1})	K_M (mM)
2AIpG	13.2 ± 0.8	1.1 ± 0.3
2AIpI	7.9 ± 0.8	8.0 ± 2.7

Fig. 4. Michaelis-Menten study of the nonenzymatic RNA copying rates of 2AIpG and 2AIpI addition across from C in the template. (*A*) Plot of k (h^{-1}) against the concentration of 2AIpI and 2AIpG. All reactions were performed at pH 8.0, 200 mM Hepes, 50 mM Mg^{2+}, 0.5 mM of activated trimer. (*B*) Michaelis-Menten parameters (V_{max} and K_M) for 2AIpG and 2AIpI. See *SI Appendix* for kinetic analysis of primer extension reactions (*SI Appendix*, Figs. S11–S24).

with U in the template (3.1 h^{-1}), and was comparable to the observed addition rates for the other canonical Watson–Crick base pairs. Interestingly, the rate of addition of I across from U in the template was slower (0.17 h^{-1}) than the rate of incorporation of G opposite U (0.58 h^{-1}; Fig. 3*C*). Primer extension with activated I across from A and I in the template was very slow, exhibiting similar behavior to activated G (Fig. 3*C*). These incorporation rates, taken together, demonstrate that I behaves similarly to G as an activated monomer, but might exhibit modestly higher fidelity because of the reduced rate of incorporation of I vs. G when paired with U in the template.

Given the comparable rates of primer extension with inosine and guanosine as monomers, we further evaluated inosine at internal positions in the template. Most important, the rate of primer extension with 2AIpC across from I in the template was similar to the rate of 2AIpI addition across from C in the template, and these rates were comparable to the rate of primer extension with 2AIpC across from G in the template (Fig. 3*C*). On the basis of the observed rates of primer extension with A, U, C, and I as activated monomers, across from inosine in the template, the projected error rate (μ_I) for copying of inosine within the template was 0.0089. This misincorporation rate was slightly lower than that calculated for both G ($\mu_G = 0.011$) and A ($\mu_A = 0.020$) within the template. Overall, a system with A, U, C, and I in the template and activated A, U, C, and I as monomers has an average projected error rate of 0.049, slightly lower than that of the corresponding system with A, U, C, and G, which has an estimated error rate of 0.066. The rates of primer extension with I and G, together with fidelity data, all indicate that I and G behave similarly, with I acting as a slightly superior nucleotide in nonenzymatic primer extension (Fig. S26).

Given the high rate of I addition across from C in the template, we evaluated the Michaelis-Menten parameters for primer extension with both G and I on a 3′-CCC-5′ template (Fig. 4). We measured primer extension rates for a range of monomer concentrations to allow estimation of V_{max} and K_M values. The K_M for 2AIpI (~8.0 mM) was approximately sevenfold higher than that of 2AIpG (~1.1 mM), whereas the V_{max} for 2AIpI and 2AIpG differed by less than twofold (7.9 and 13.2 mM·h^{-1}, respectively). The estimated catalytic efficiency (V_{max}/K_M) was an order of magnitude higher for guanosine relative to inosine across from cytidine, primarily because of the tighter binding of the activated guanosine mononucleotide.

Effect of 8-Oxo-Purines and Inosine at the 3′-End of the Primer. Previous reports indicate that the rate of primer extension is strongly dependent on the nature of the last primer–template base pair. A factor of 30–200-fold rate decrease has been observed for non-Watson–Crick, nonwobble base pairs at the 3′ end of 3′-amino-2′,3′-dideoxynucleotide-terminated primers (15). Because of this potentially large effect, we explored the influence of noncanonical bases at the 3′-end of the primer. We therefore measured the rate of nonenzymatic RNA primer extension using RNA primers containing either 8-oxo-purines or inosine at the 3′-terminus, opposite all four canonical nucleotides in the template. In each case, we measured the rate of primer extension, using 2AIpG as the monomer on a 3′-CCC-5′ template. Because G is incorporated efficiently on an oligo-C template, no downstream-activated helper oligonucleotide was used (Fig. 5*A*). Stalling factors (*S*), the ratio of the rate of primer extension with Watson–Crick pair divided by the rate of primer extension with a mismatched pair, were calculated. For example, the stalling factor for primer extension beyond a 3′-terminal inosine in a terminal C:I pair is calculated as $S_{C:I} = k_{C:G}/k_{C:I}$, where $k_{C:G}$ is the extension rate beyond a C:G pair, and $k_{C:I}$ is the extension rate beyond the C:I pair (see *Materials and Methods* for additional details) (15). A higher value corresponds to increased stalling resulting from the 3′-terminal primer–template pair. A primer terminated with inosine at the 3′ position gave a minimal stalling factor of 1.3 when the inosine could form a Watson–Crick C:I pair with C in the template. Stalling factors for I and G opposite the wobble-pairing partner U were similar, at 1.8 and 0.57. Stalling factors for inosine were much higher for all other non-Watson–Crick pairs (Fig. 5*B*).

A

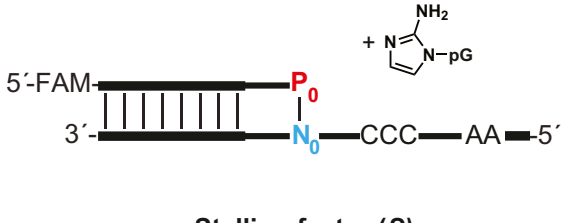

B

Stalling factor (*S*)

N_0 \ P_0	8OxA	8OxG	I	G
A	32(1)	6.9(5)	8.2(6)	15(1)
U	24(4)	39(6)	1.8(3)	0.57(4)
G	55(4)	32(2)	320(8)	14(1)
C	46(2)	12(1)	1.3(1)	1

Fig. 5. (*A*) Schematic representation of nonenzymatic primer extension with a primer that contains a noncanonical nucleotide (P_0) 3′ end. (*B*) Stalling factors ($S_{P:N}$) of nonenzymatic RNA polymerization of 2AImpG. See *SI Appendix* for kinetic analysis of primer extension reactions (*SI Appendix*, Figs. S27–S36).

In contrast to the favorable properties of inosine, primer extension rates for primers with 3′-terminal 8-oxo-purines were much slower, with stalling factors of 6.9–55. When 8-oxo-purines are paired across the corresponding Watson–Crick nucleotide in the template, the stalling factors were 12 and 24 for 8-oxo-G and 8-oxo-A, respectively. When the template nucleotide could potentially form a Hoogsteen base pair with the nucleotide at the end of the primer (A:8OxG and G:8OxA, for instance), high stalling factors were also observed. These results suggest that 8-oxo-purine monomers would not be functional components of a nonenzymatic RNA copying system; not only are the 8-oxo-purine monomers very poor substrates for primer extension, but if they are incorporated, they strongly inhibit the next step of primer extension.

Discussion

We have found that two different classes of noncanonical nucleotides, 8-oxo-purines and inosine, behave very differently in nonenzymatic primer extension. Three separate lines of evidence suggest that the 8-oxo-purines are unlikely to have been a functional component of a primitive RNA-based genetic system: the incorporation of the 8-oxo-purine monomers in helper-assisted primer extension is kinetically slow, and in the rare cases where an 8-oxo-purine residue is incorporated at the 3′ end of a primer, subsequent primer extension is also very slow. In addition, 8-oxo-adenosine in a template leads to slow primer extension with U, whereas 8-oxo-guanosine in a template results in highly error prone primer extension. It is known that the 8-oxo-modified purine nucleotides have different proportions of glycosidic conformations (*syn* vs. *anti*) relative to their canonical counterparts (30). We believe that the poor primer extension observed for the 8-oxo purines may be a direct result of this conformational state. Oxidative damage of the standard purines in a template strand would be strongly deleterious and conditions that promote extensive guanosine oxidation would likely be incompatible with the emergence of functional RNAs from nonenzymatic RNA replication.

In contrast to the 8-oxo-purines, inosine behaves as a reasonable monomer in nonenzymatic RNA primer extension. As an activated monomer, it is incorporated with a rate comparable to that of guanosine, and the I:C base pair at the end of a primer exhibits a minimal stalling effect. In the template, I was copied with a rate and fidelity similar to that of G. The fidelity with which a template that contained I (AUIC) was copied with A, U, C, and I monomers (error frequency, 0.049) was slightly better than that with which an AUCG template would be copied with A, U, C, and G as monomers (error frequency, 0.066). Interestingly, the fidelity of the mixed system in which A, U, C, and I monomers are copying an AUGC template was similar, with an error rate of ∼0.050. The mixed system in which A, U, C, and G monomers are copying an A, U, I, C template had a slightly higher misincorporation rate of ∼0.075 (*SI Appendix*, Fig. S25). The fidelity of RNA copying with inosine in place of guanosine requires further study, as both sequence context and reaction conditions such as nucleotide concentrations are likely to affect the error rates. For example, fidelity might be significantly improved simply because of competition for binding to the template when all four monomers are present together. In addition, the stalling effect will certainly increase the fidelity of the most rapidly completed copies of a template. Assuming that purine–purine mismatches essentially permanently stall primer extension, while ignoring the minimal stalling observed for wobble-pairs, an estimated overall error rate for the A, U, C, and I system was calculated to be 0.024. These assumptions have a smaller effect on the estimated error rate A, U, C, G system (0.050), where errors are dominated by G:U wobble pairing (*SI Appendix*, Fig. S26).

Orgel and coworkers previously studied nonenzymatic primer extension with inosine, and reported poor copying of dC-rich templates with 2-methylimidazole-activated inosine (13). In addition, cytidine activated with 2-methylimidazole showed negligible primer extension across from inosine on a DNA template (12). Our results differ significantly from these earlier observations. However, there are several important differences in the conditions in which template-directed synthesis experiments were carried out. Notably, as first described by Orgel and coworkers (31), template-directed polymerization of activated RNA mononucleotides is more efficient on RNA templates (e.g., our current work using an RNA primer–template duplex) relative to DNA templates (e.g., previous work on inosine by Orgel's group). Moreover, our primer extension reactions made use of activated trimer helpers to further catalyze the reaction. Last, we used a superior leaving group, 2-aminoimidazole, for our primer extension reactions, whereas previous work was carried out using the less effective 2-methylimidazole leaving group. Our optimized conditions for RNA copying may have more prebiotic relevance, given that our group has previously described a prebiotically plausible synthesis of 2-aminoimidazole (32).

Previous work from our laboratory has shown that s^2U or s^2rT in place of U can lead to substantial improvements in fidelity. Future work should address the fidelity of template copying in systems that contain these and other modified nucleotides. Nevertheless, our current observations suggest that the primordial genetic polymer could have been a version of RNA in which inosine took the place of guanosine, either partially or completely.

One of the key challenges in nonenzymatic RNA replication is strand separation, which is necessary to propagate RNA replication. RNA duplexes of 30–50 nucleotides are extremely thermostable, making RNA strand separation a significant challenge (33). Thus, factors that lower the melting temperature of RNA duplexes without compromising RNA copying are of considerable interest. The weaker I:C base pairs formed as a result of template copying would decrease the overall melting temperature of the product duplex. Previous reports indicate that substituting guanosine with inosine decreases the stability of RNA duplexes by 3.44 kcal/mol per G:C to I:C change, primarily because of the lack of hydrogen bonding to the C2-carbonyl of cytidine (34). With inosine in place of guanosine, long RNA duplexes will have lower melting temperatures, and thus, inosine could potentially facilitate RNA replication via thermal cycling.

Our results inform the constraints we place on the prebiotic synthesis of nucleotides, because just as the pathway to C also provides U by deamination, so a pathway to A could also provide I by deamination. Although the spontaneous deamination of A to I is very slow, this conversion is greatly accelerated by the presence of nitrous acid, which in turn can be derived from atmospherically generated NO, or NO from cometary impacts. It has recently been proposed that dilute atmospherically derived NO could be concentrated by coordination with ferrocyanide complexes in the form of nitroprusside, which in turn could serve as a starting material for isonitrile-mediated nucleotide activation with 2-aminoimidazole (35). A dual role for NO in nucleotide activation chemistry, and more directly in nucleotide synthesis through the deamination of adenosine to inosine, would be a satisfyingly parsimonious systems approach to both the origin of RNA and RNA replication. Assuming that sufficient I can be derived from A, the search for a prebiotically plausible path to the purine nucleotides need not extend beyond the identification of a path to the synthesis of adenosine.

Materials and Methods

The primer–template duplex was first annealed in a solution of 50 mM NaCl, 50 mM Na-HEPES at pH 8.0, and 1 mM Na_2EDTA, by heating at 95 °C for 1 min and then cooling down to 25 °C at a rate of 0.1 °C/s. The primer–template mixture was diluted fourfold into a solution containing 50 mM $MgCl_2$ and 200 mM Na-HEPES at pH 8.0. The reaction mixture was initiated by adding 20 mM activated monomer. If a trimer helper was used in the reaction, it was added at a 0.5 mM concentration. Aliquots (1 μL each) were removed and were mixed with 29 μL quenching buffer containing 12.5 mM EDTA, 75 μM complementary strand in 90% formamide solution. These quenched samples were heated at 95 °C for 1 min, and 3 μL aliquot was separated by 20% denaturing PAGE gel with 7 M urea. The gel was scanned using a Typhoon 9410

scanner, and the bands were quantified using ImageQuant TL software. Detailed experimental protocols are provided in *SI Appendix*.

ACKNOWLEDGMENTS. We thank Constantin Giurgiu, Daniel Duzdevich, and James Tam for their helpful discussions. We also thank the entire J.W.S. group for feedback. J.W.S. is an investigator of the Howard Hughes Medical Institute. This work was supported in part by a grant from the Simons Foundation (290363 to J.W.S.) and by a grant from the National Science Foundation (CHE-1607034 to J.W.S.). D.K.O. is a recipient of a Postdoctoral Research Scholarship (B3) from the Fonds de recherche du Québec–Nature et technologies, Quebec, Canada, and a postdoctoral fellowship from Canadian Institutes of Health Research from Canada.

1. Woese CR (1967) *The Genetic Code: The Molecular Basis for Genetic Expression* (Harper & Row, New York).
2. Crick FH (1968) The origin of the genetic code. *J Mol Biol* 38:367–379.
3. Orgel LE (1968) Evolution of the genetic apparatus. *J Mol Biol* 38:381–393.
4. Cafferty BJ, Fialho DM, Khanam J, Krishnamurthy R, Hud NV (2016) Spontaneous formation and base pairing of plausible prebiotic nucleotides in water. *Nat Commun* 7:11328.
5. Sutherland JD, Whitfield JN (1997) Prebiotic chemistry: A bioorganic perspective. *Tetrahedron* 53:11493–11527.
6. Powner MW, Gerland B, Sutherland JD (2009) Synthesis of activated pyrimidine ribonucleotides in prebiotically plausible conditions. *Nature* 459:239–242.
7. Stairs S, et al. (2017) Divergent prebiotic synthesis of pyrimidine and 8-oxo-purine ribonucleotides. *Nat Commun* 8:15270.
8. Szostak JW (2017) The narrow road to the deep past: In search of the chemistry of the origin of life. *Angew Chem Int Ed Engl* 56:11037–11043.
9. Engelhart AE, Powner MW, Szostak JW (2013) Functional RNAs exhibit tolerance for non-heritable 2′-5′ versus 3′-5′ backbone heterogeneity. *Nat Chem* 5:390–394.
10. Trevino SG, Zhang N, Elenko MP, Lupták A, Szostak JW (2011) Evolution of functional nucleic acids in the presence of nonheritable backbone heterogeneity. *Proc Natl Acad Sci USA* 108:13492–13497.
11. Heuberger BD, Pal A, Del Frate F, Topkar VV, Szostak JW (2015) Replacing uridine with 2-thiouridine enhances the rate and fidelity of nonenzymatic RNA primer extension. *J Am Chem Soc* 137:2769–2775.
12. Kozlov IA, Orgel LE (1999) Nonenzymatic oligomerization reactions on templates containing inosinic acid or diaminopurine nucleotide residues. *Helv Chim Acta* 82: 1799–1805.
13. Rembold H, Robins RK, Seela F, Orgel LE (1994) Polycytidylate and poly(7-deazaguanylate): A pair of complementary templates. *J Mol Evol* 38:211–214.
14. Robertson MP, Joyce GF (2012) The origins of the RNA world. *Cold Spring Harb Perspect Biol* 4:a003608.
15. Rajamani S, et al. (2010) Effect of stalling after mismatches on the error catastrophe in nonenzymatic nucleic acid replication. *J Am Chem Soc* 132:5880–5885.
16. Ferré-D'Amaré AR, Scott WG (2010) Small self-cleaving ribozymes. *Cold Spring Harb Perspect Biol* 2:a003574.
17. Kun A, Santos M, Szathmáry E (2005) Real ribozymes suggest a relaxed error threshold. *Nat Genet* 37:1008–1011.
18. Garmendia C, Bernad A, Esteban JA, Blanco L, Salas M (1992) The bacteriophage phi 29 DNA polymerase, a proofreading enzyme. *J Biol Chem* 267:2594–2599.
19. Natrajan G, et al. (2003) Structures of Escherichia coli DNA mismatch repair enzyme MutS in complex with different mismatches: A common recognition mode for diverse substrates. *Nucleic Acids Res* 31:4814–4821.
20. Leu K, Obermayer B, Rajamani S, Gerland U, Chen IA (2011) The prebiotic evolutionary advantage of transferring genetic information from RNA to DNA. *Nucleic Acids Res* 39:8135–8147.
21. Larsen AT, Fahrenbach AC, Sheng J, Pian J, Szostak JW (2015) Thermodynamic insights into 2-thiouridine-enhanced RNA hybridization. *Nucleic Acids Res* 43:7675–7687.
22. Crick FH (1966) Codon–Anticodon pairing: The wobble hypothesis. *J Mol Biol* 19: 548–555.
23. Cadet J, Douki T, Ravanat JL (2008) Oxidatively generated damage to the guanine moiety of DNA: Mechanistic aspects and formation in cells. *Acc Chem Res* 41: 1075–1083.
24. Choi YJ, Chang SJ, Gibala KS, Resendiz MJE (2017) 8-Oxo-7,8-dihydroadenine and 8-Oxo-7,8-dihydroadenosine-chemistry, structure, and function in RNA and their presence in natural products and potential drug derivatives. *Chemistry* 23:6706–6716.
25. Prywes N, Blain JC, Del Frate F, Szostak JW (2016) Nonenzymatic copying of RNA templates containing all four letters is catalyzed by activated oligonucleotides. *eLife* 5:e17756.
26. Walton T, Szostak JW (2016) A highly reactive imidazolium-bridged dinucleotide intermediate in nonenzymatic RNA primer extension. *J Am Chem Soc* 138:11996–12002.
27. Tam CP, et al. (2017) Downstream oligonucleotides strongly enhance the affinity of GMP to RNA primer–template complexes. *J Am Chem Soc* 139:571–574.
28. Li L, et al. (2017) Enhanced nonenzymatic RNA copying with 2-aminoimidazole activated nucleotides. *J Am Chem Soc* 139:1810–1813.
29. Frelon S, Douki T, Favier A, Cadet J (2002) Comparative study of base damage induced by gamma radiation and Fenton reaction in isolated DNA. *J Chem Soc Perkin Trans 1* 24:2866–2870.
30. Choi YJ, Chang SJ, Gibala KS, Resendiz MJE (2017) 8-Oxo-7,8-dihydroadenine and 8-Oxo-7,8-dihydroadenosine—Chemistry, structure, and function in RNA and their presence in natural products and potential drug derivatives. *Chemistry* 23:6706–6716.
31. Zielinski M, Kozlov IA, Orgel LE (2000) A comparison of RNA with DNA in template-directed synthesis. *Helv Chim Acta* 83:1678–1684.
32. Fahrenbach AC, et al. (2017) Common and potentially prebiotic origin for precursors of nucleotide synthesis and activation. *J Am Chem Soc* 139:8780–8783.
33. Siegfried NA, Kierzek R, Bevilacqua PC (2010) Role of unsatisfied hydrogen bond acceptors in RNA energetics and specificity. *J Am Chem Soc* 132:5342–5344.
34. Szostak JW (2012) The eightfold path to non-enzymatic RNA replication. *J Syst Chem* 3:2.
35. Mariani A, Russell DA, Javelle T, Sutherland JD (2018) A light-releasable potentially prebiotic nucleotide activating agent. *J Am Chem Soc* 140:8657–8661.